CrossMark

ARTICLE

3D modelling and sheath folding at the Falun pyritic Zn-Pb-Cu-(Au-Ag) sulphide deposit and implications for exploration in a 1.9 Ga ore district, Fennoscandian Shield, Sweden

Tobias C. Kampmann[1] · Michael B. Stephens[1,2] · Pär Weihed[1]

Abstract Altered and mineralized rocks at the Falun pyritic Zn-Pb-Cu-(Au-Ag) sulphide deposit, situated in the Palaeoproterozoic Bergslagen ore district in the southwestern part of the Fennoscandian Shield, have been metamorphosed at low-pressure, amphibolite-facies conditions and affected by ductile deformation. Using combined surface mapping of lithology and structure, drill core logging and microstructural work, the polyphase (D_1 and D_2) ductile deformation is demonstrated and a 3D model for the deposit created. Mineral associations include quartz, biotite, cordierite, anthophyllite, and minor almandine, andalusite and chlorite in silicate-rich altered rock, calcite or dolomite in marble and tremolite-actinolite or diopside-hedenbergite in skarn. The silicate minerals show varying growth patterns during the different phases of the tectonothermal evolution, with considerable static grain growth occurring between D_1 and D_2, and even after D_2. F_2 sheath folding along axes that plunge steeply to the SSE, parallel to a mineral stretching lineation and the dip direction of the S_2 foliation, is suggested as a key deformation mechanism forming steeply plunging, cone- to rod-shaped mineralized bodies. This contrasts with a previous structural model invoking fold interference. A major shear zone with talc-chlorite-(quartz-biotite) mineral association separates the northern and southern structural domains at the deposit and bounds the polymetallic massive sulphides to the north.

Introduction

The Bergslagen ore district in south-central Sweden (Fig. 1a) is host to a large number of iron oxide and base metal sulphide deposits, some of which contain significant gold and silver contents (Stephens and Weihed 2013). The Falun pyritic Zn-Pb-Cu-(Au-Ag) sulphide deposit in the northern part of the district (Fig. 1a) was the most important base metal producer in Sweden. Mining operations were carried out for about 1000 years until 1992, with a calculated total production of approximately 28–35 Mt of ore at average grades of up to 5 % Zn, 2 % Pb, 0.6–4 % Cu, 13–35 g/t Ag and 0.5–4 g/t Au (Tegengren 1924; Grip 1978; Allen et al. 1996).

Falun has been interpreted historically as one of the type examples of deformed and metamorphosed base metal sulphide deposits in the Bergslagen ore district (Fig. 1a). Earlier studies distinguished between Falun- and Åmmeberg-type ores, relating their formation to contact-metasomatic processes associated with the emplacement of ~1.9 Ga intrusions and migmatization associated with the emplacement of ~1.8 Ga intrusions, respectively (Geijer 1917, 1964; Magnusson, 1950, 1953). Based mainly on volcanic setting and host rock characteristics, Allen et al. (1996) classified the base metal sulphide deposits in the Bergslagen ore district as stratabound volcanic-associated limestone-skarn (SVALS) and stratiform ash-siltstone-hosted (SAS) deposits. Both were regarded to have formed in a submarine environment during the waning
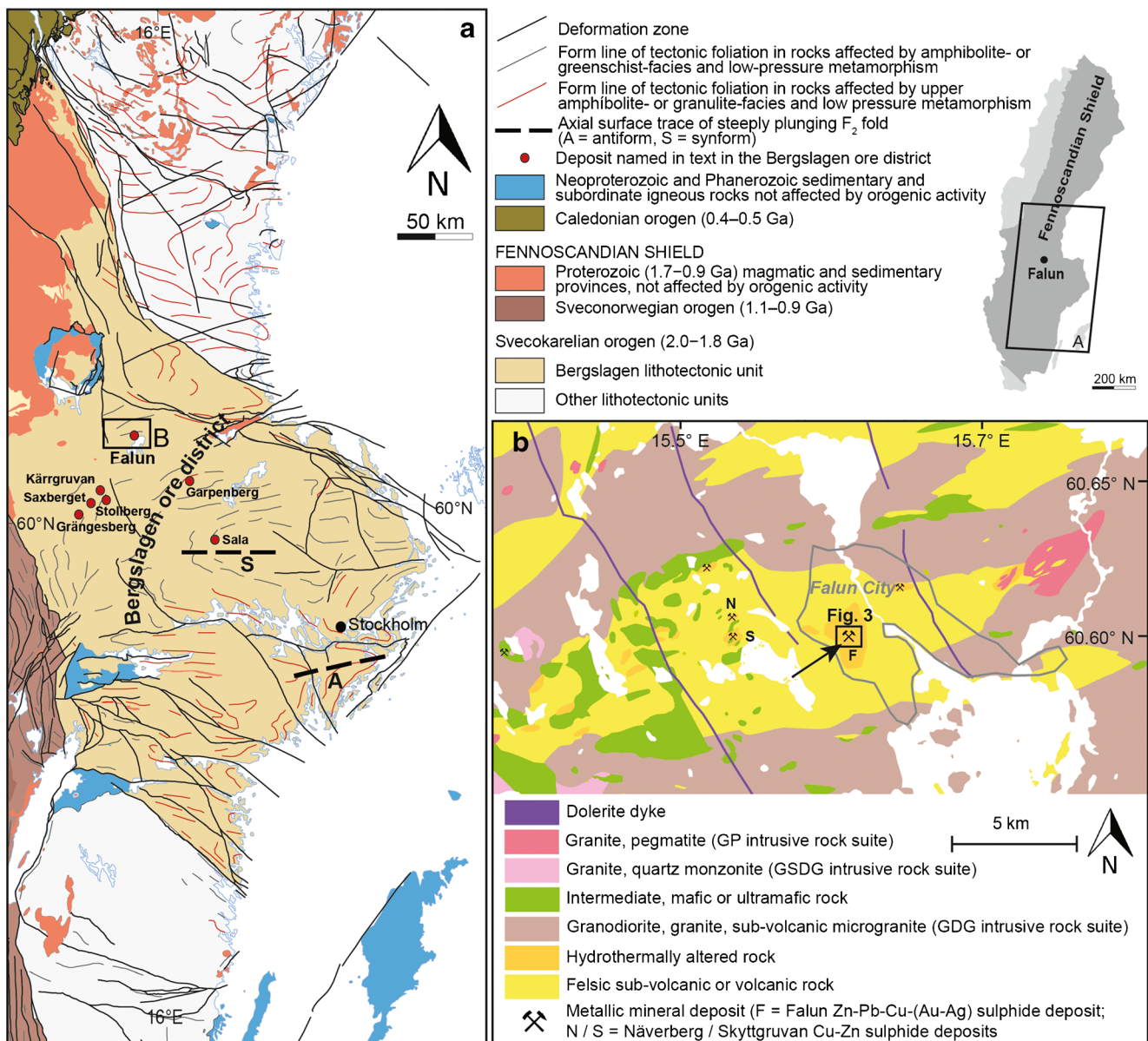
✉ Tobias C. Kampmann
  tobias.kampmann@ltu.se

1   Department of Civil, Environmental and Natural Resources Engineering, Luleå University of Technology, SE-971 87 Luleå, Sweden

2   Geological Survey of Sweden, Box 670, SE-751 28 Uppsala, Sweden

Fig. 1 **a** Lithotectonic map of the south-western part of the Fennoscandian Shield in Sweden, showing the spatial distribution of major lithotectonic units, structural form line patterns and mineral deposits. Rock types and structures within the Bergslagen lithotectonic unit are described in the text (modified from Stephens and Andersson 2015). **b** Lithological map of the Falun inlier, modified after recent geological mapping by the Geological Survey of Sweden

stage of a period of intense, mainly felsic volcanism, prior to metamorphism and deformation. In this classification, the Falun deposit is a SVALS deposit, similar to the operating mine at Garpenberg and other deposits at Sala, Saxberget and Stollberg (Fig. 1a).

This paper describes a new model for the distribution of metamorphosed mineralization types and altered rocks at the Falun deposit, based on a study of the polyphase ductile deformation. Field data collected from the open pit have been combined with drill core logging, and legacy 2D mine maps and mine sections to create a three-dimensional model of the mine. Microstructural analysis has been used to further

characterize the ductile deformation and the relative timing of mineral growth or recrystallization and deformation in the metamorphosed altered rocks.

Geological setting

Regional geological setting

The Bergslagen ore district is located inside the Bergslagen lithotectonic unit in the south-western part of the Svecokarelian orogen, Fennoscandian Shield, Sweden

(Fig. 1; Stephens et al. 2009, Stephens and Andersson 2015). The 2.0–1.8 Ga Svecokarelian orogeny in this lithotectonic unit involved two tectonic cycles, from 1.91–1.86 Ga and 1.86–1.82 Ga, dominated by transtensional or extensional deformation (Stephens et al. 2009; Beunk and Kuipers 2012; Stephens and Andersson 2015). Transpressive deformation occurred around 1.87–1.86 Ga (Hermansson et al. 2007, 2008a; Stephens et al. 2009; Stephens and Andersson 2015) and 1.84–1.82 Ga (Beunk and Kuipers 2012, Stephens and Andersson 2015), during the waning stages of each cycle. Subsequent ductile strain was restricted to shear zones (Hermansson et al. 2008b). These tectonic processes occurred along an active continental margin and included metamorphism under low-P, greenschist- to amphibolite-, locally even granulite-facies conditions (Hermansson et al. 2008a; Stephens et al. 2009).

Megascopic sheath folding (F_2) deforming a planar ductile grain-shape fabric (S_1) has been identified inside a steeply dipping, dextral strike-slip shear belt with WNW–ESE trend in the north-east of the Bergslagen lithotectonic unit (Fig. 1; Stephens et al. 2009). Falun lies inside the structural domain to the south-west of this shear belt, on the north-western limb of a major, E-plunging, F_2 synform (Fig. 1a). Tight to isoclinal F_2 folds on different scales with an E–W to NE–SW axial surface trace and steeply dipping, ductile shear zones with a similar strike dominate this domain (Stephens et al. 2009; Beunk and Kuipers 2012).

The vast majority of the iron oxide and base metal sulphide deposits in Bergslagen, including Falun, are hosted by metamorphosed, 1.91–1.89 Ga felsic volcanic and sub-volcanic rocks, in close spatial association with marble and skarn (Allen et al. 1996; Stephens et al. 2009). This succession was both preceded and followed by the sedimentation of siliciclastic rocks. It has previously been demonstrated that altered rocks associated with base metal sulphide deposits at Falun (Wolter and Seifert 1984) and in other deposits in the Bergslagen ore district (Trägårdh 1991; Allen et al. 1996; Stephens et al. 2009) are metamorphosed equivalents to hydrothermally altered rocks. The term 'altered rocks' in this paper refers to hydrothermally altered rocks at the Falun deposit that have undergone later tectonic overprint; they are named according to their current metamorphic mineralogy.

Large volumes of plutonic rocks intruded the supracrustal sequence. An older 1.90–1.87 Ga intrusive suite with a calc-alkaline geochemical trend, referred to as the granitoid rock-diorite-gabbro (GDG) intrusive rock suite, crystallized prior to the tectonic overprint in the Bergslagen lithotectonic unit. Younger plutonic rocks belonging to 1.87–1.84 Ga and 1.81–1.78 Ga granite-granodiorite-syenitoid rock-quartz monzodiorite-gabbro (GSDG) intrusive suites, with an alkali-calcic trend, crystallized after the development of some ductile deformation but are affected, at least in part, by later ductile strain. A uniform granite-pegmatite (GP) intrusive rock suite formed during the same time interval as the GSDG suites.

Local geological setting

The Falun deposit is located inside an inlier of metamorphosed, felsic sub-volcanic and volcanic rocks, surrounded by mainly metamorphosed, coarse-grained granite and microgranite belonging to the GDG intrusive suite (Fig. 1b). Bromley-Challenor (1988) suggested stratigraphic younging from north to south inside the inlier but did not consider the effects of isoclinal folding and ductile shearing. The sub-volcanic and volcanic rocks are intruded by mafic and ultra-mafic rocks (Fig. 1b), some of which are folded, affected by a steep mineral lineation and belong to the GDG intrusive suite. Younger felsic intrusive rocks belonging to the GSDG and GP suites are also present around the inlier (Fig. 1b).

The deposit is spatially associated with a zone of hydro-thermally altered rocks, which extends over an area of several thousand square metres at the ground surface (Fig. 1b). As a consequence of ductile deformation and metamorphism at peak metamorphic P/T conditions of 2.5 ± 1 kbar and 550 ± 50 °C (Wolter and Seifert 1984), the hydrothermally altered rocks were converted to rocks rich in quartz and mica with porphyroblasts of cordierite, amphibole and garnet, traditionally referred to as 'ore quartzite' and 'mica schist' (Geijer 1917). Dolomite and calcite marble as well as skarn occur as subordinate lithologies, both as separate rock units and as relic fragments in the pyritic massive sulphides.

The Falun deposit and the associated altered rocks are folded by a large-scale steeply SSE-plunging synform (Weijermars 1987, unpublished mine report). Pyritic massive sulphides are thickened and concentrated in the hinge to the fold and continue down to an elevation of approximately 450 m beneath sea level (−450 m). Other types of mineralization include (1) disseminated to semi-massive Cu-Au mineralization in quartz-rich altered rock hosting Au-bearing quartz veins on the eastern side of the deposit; (2) sulphide-bearing, typically 0.5–2-m-thick ductile shear zones; and (3) minor Zn-Pb-bearing skarn. Åberg and Fallick (1993) concluded that the Au-bearing quartz veins formed after the base metal massive sulphides.

Method of approach

Field and core logging studies

Field studies were carried out in the open pit, road cuts and other outcrops close (<1 km) to the Falun mine. The mapping in the open pit was limited by the non-accessibility of the medium- and high-level benches. In addition, samples were

taken from drill cores archived at the Geological Survey of Sweden's national archive in Malå, Sweden. More recent drill cores by Drake Resources Ltd. were also made available for investigation. In total, 35 drill cores totalling ~3600 m were investigated for the present study.

Analysis of microstructures

Both oriented and non-oriented samples of metamorphosed, felsic sub-volcanic or volcanic rocks surrounding the deposit and different types of rock inside the hydrothermally altered zone were collected. Polished thin sections were studied to identify mineral associations and microstructures and establish the structural relationships between the growth of minerals and ductile deformation features. In addition, textural studies on a smaller scale and semi-quantitative mineral chemistry analyses were performed using a field emission scanning electron microscope (Merlin Zeiss Gemini) at Luleå University of Technology, Sweden, equipped with an energy-dispersive X-ray spectrometer.

3D modelling

A 3D geological model was created to visualize the geometry of the lithologies, especially the mineralized bodies at depth. The spatial dimensions of the model block are 800 m in an E–W horizontal direction, 550 m in a N–S horizontal direction and 600 m in a vertical direction (approximately +150 to −450 m). The current surface at the Falun deposit lies at approximately +150 m outside and +30 m in the central part of the open pit. The different mineralized bodies have been modelled from this surface down to −450 m, which represents the location of the deepest available mine map. By contrast, the altered rocks and other lithologies have been modelled down to +30 m, i.e. down to the base of the open pit. The simplistic mapping of altered rocks on the mine maps, along with the paucity of sufficient drill core data to make assumptions on the 3D geometry of these rocks, did not allow modelling of these rocks down to the full vertical extent of the model.

The ground surface in the 3D model is based on a high-resolution ($25/100$ m^2 point measurement density) digital elevation model and satellite images provided by the Ordnance Survey of Sweden. Construction of the 3D model for the Falun deposit was carried out using 140 legacy level maps from different horizontal sections and elevations in the mine as well as accompanying vertical cross sections. The maps and sections mainly show the spatial distribution of different mineralization types along mine adits and boreholes, and the extent of the different mineralized bodies at the deposit. However, large areas at depth have not been mapped due to the uneven distribution of adits and boreholes. The mine maps were georeferenced into the coordinate system SWEREF99

and imported into the 3D modelling software GOCAD 2009.3 (Paradigm Ltd.), including the SPARSE-plugin (Mira Geosciences Ltd.).

The surface geological map of the Falun deposit, as discussed below, forms the basis for modelling the geometry of the different lithologies to depth. The shapes of the rock units on this map were initially outlined and projected onto a digital elevation model. Subsequently, the horizontal shapes of the different mineralization types and the available spatial distribution data for the altered rocks at the respective depths on the mine maps were outlined and vertically connected, defining the outer boundaries of the rock bodies as 3D surfaces (Fig. 2). The altered rocks and other lithologies were projected down using the structural measurements collected at surface. To test the spatial relationship between a major ductile shear zone in the northern part of the deposit and the mineralized bodies, the shear zone was computed down to the base of the 3D model, using the extrapolation of structural measurements at surface and the identification of this zone in the core data.

Where necessary, the geometry of the rock units was modified to avoid unreasonable cross-cutting relationships. Cross-cutting relationships were only permitted for porphyritic felsic dykes and for the massive, pyritic Zn-Pb-Cu-rich and Cu-rich sulphides. In addition, cross-cutting relationships between massive, pyritic Cu-rich sulphides and the ductile shear zone in the northern part of the open pit were modelled. The positions of 610 drill holes were calculated with trigonometric functions using spatial information included in the mine data. Lithological and contact information from the drill core investigations carried out in this study was then used to verify and refine the 3D model at different depths (Fig. 2). In particular, the intersections of mineralization in the drill cores, mapped during core logging, were compared with the intersection of the mineralized bodies and the drill cores in the 3D model to validate or, if necessary, modify the model. The uneven distribution of available drill core, including, for example, the lack of available drill cores on the western and southwestern sides of the deposit and at depth (Fig. 2), limited this validation procedure.

Results

Spatial distribution of rock units at the ground surface

Altered rocks and late- or post-sulphide dykes

Silicate-rich altered rocks form the most abundant lithology in the metamorphosed, hydrothermally altered zone at the Falun deposit (Fig. 3). They are characterized by the mineral association of quartz-anthophyllite-(biotite-cordierite/almandine), biotite-quartz-cordierite-(anthophyllite) and biotite-cordierite/
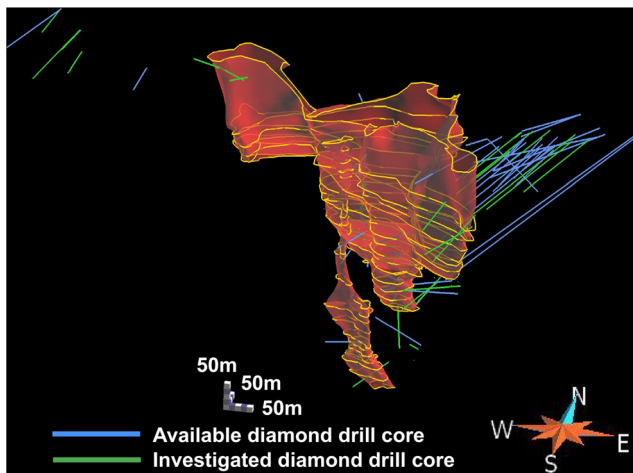
Fig. 2 Locations of available and mapped drill cores at the Falun deposit, used to validate the 3D model

almandine, herein referred to as QA rock, and BQC and BCA schists, respectively, emphasizing also differences in foliation penetrativity. The biotite commonly shows Mg/(Mg + Fe) ratios exceeding 0.8.

The QA rock is medium-grained and equigranular and has a modal composition of ~65 to 80 % quartz, 10 % anthophyllite, either cordierite or fractured and retrogressed almandine (up to 10 %), sulphide minerals (pyrite and chalcopyrite, up to 10 %) and variable contents of biotite. Andalusite, magnetite, cummingtonite and gahnite ($ZnAl_2O_4$) porphyroblasts are minor components. The BQC schist has an equigranular groundmass of medium-grained biotite (50 %), quartz (25 %) and anthophyllite (5 %). The biotite is typically associated and intergrown with medium- to coarse-grained, elongate (up to 100 mm) cordierite porphyroblasts (20 %). Cordierite is usually pinitized, has a yellow-brown appearance and contains quartz and mica inclusions. The BCA schist is characterized by very low quartz content and usually coarse-grained (up to 15 mm) biotite (70–80 %). Cordierite or, in some units, almandine, which is typically strongly fractured and retrogressed and lacks inclusions, is present. In all silicate-rich altered rocks, chlorite is common (up to 20 %), both as a retrograde product after cordierite and as fine veins and fracture filling. Although significant concentrations are restricted to the QA rock, both chalcopyrite and pyrite can also occur as minor phases in the BQC and BCA schists.

Calcite or dolomite marble, skarn and tremolite-quartz-sericite schist form subordinate lithologies at the Falun deposit (Fig. 3). The skarns contain diopside-hedenbergite or tremolite-actinolite, the former commonly spatially associated with calcite marble. In the south-eastern part of the open pit, ~5-mm-thick, alternating bands of diopside-hedenbergite skarn and calcite marble are present. Furthermore, in drill core samples, diopside-hedenbergite skarn with minor hornblende and garnet occurs, the latter dominated by the cations Fe, Ca and minor Mg and Mn. Medium- to coarse-grained tremolite is a

characteristic mineral in the tremolite-actinolite skarn, which has only been identified in the drill cores. Tremolite-quartz-sericite schist occurs close to the contact between massive pyritic sulphides and dolomite marble or between QA rock and amphibolite.

Dykes with a felsic composition and porphyritic texture, varying in thickness from ~2 to 10 m, are abundant in the hydrothermally altered zone at the Falun deposit (Fig. 3). The groundmass in the dykes is fine- to medium-grained and consists mainly of quartz, plagioclase, biotite, muscovite and K-feldspar. Magnetite occurs as an accessory phase. Recrystallized phenocrysts of mainly quartz, but also plagioclase and minor K-feldspar, are abundant (10–20 %). As this rock type does not contain cordierite, anthophyllite or almandine, characteristic of the silicate-rich altered rocks, the dykes are inferred to have been less intensely altered, suggesting that they intruded at a late stage of and/or after the alteration and sulphide mineralization event.

Dyke-like bodies of amphibolite with thicknesses of ~0.5 m containing cummingtonite and/or hornblende (70 %) and minor magnetite, biotite, quartz and plagioclase have been observed inside the hydrothermally altered zone. Observations in drill cores and on the legacy mine maps indicate that these amphibolites occasionally form ~0.2–1-m-thick rims around the porphyritic felsic dykes (Fig. 3). A possibly composite dyke relationship between dominant felsic and subordinate mafic components is inferred.

Types of mineralization

Different mineralization types are completely surrounded by the hydrothermally altered zone at Falun (Fig. 3). Cu-Au mineralization is characterized by medium- to coarse-grained chalcopyrite and pyrite with minor pyrrhotite and sphalerite, often forming veinlet-like networks in the QA rock. This mineralization type varies from disseminated to semi-massive types (Fig. 3) with average metal head grades of ~3–4 % Cu and 2 g/t Au (Grip 1978). The Au-bearing quartz veins described by Åberg and Fallick (1993) also occur in the QA rock.

Massive, pyritic Cu-rich and Zn-Pb-Cu-rich sulphides are transitional to each other in the central part of the deposit (Fig. 3). Pyrite and less commonly pyrrhotite are typically the dominant sulphide minerals (40–60 %) in both massive sulphide types. Chalcopyrite is the main sulphide mineral in the Cu-rich massive sulphides while sphalerite, galena and chalcopyrite are characteristic minerals in the Zn-Pb-Cu-rich massive sulphides. For the massive sulphides as a whole, average head grades of 5 % Zn, 1.7 % Pb, 0.7 % Cu, 35 g/t Ag and 0.5 g/t Au were reported (Grip 1978).

Lower-grade mineralization consisting of mostly chalcopyrite and pyrite, but also galena and sphalerite, is present in ductile shear zones at the deposit. Minor mineralized skarn
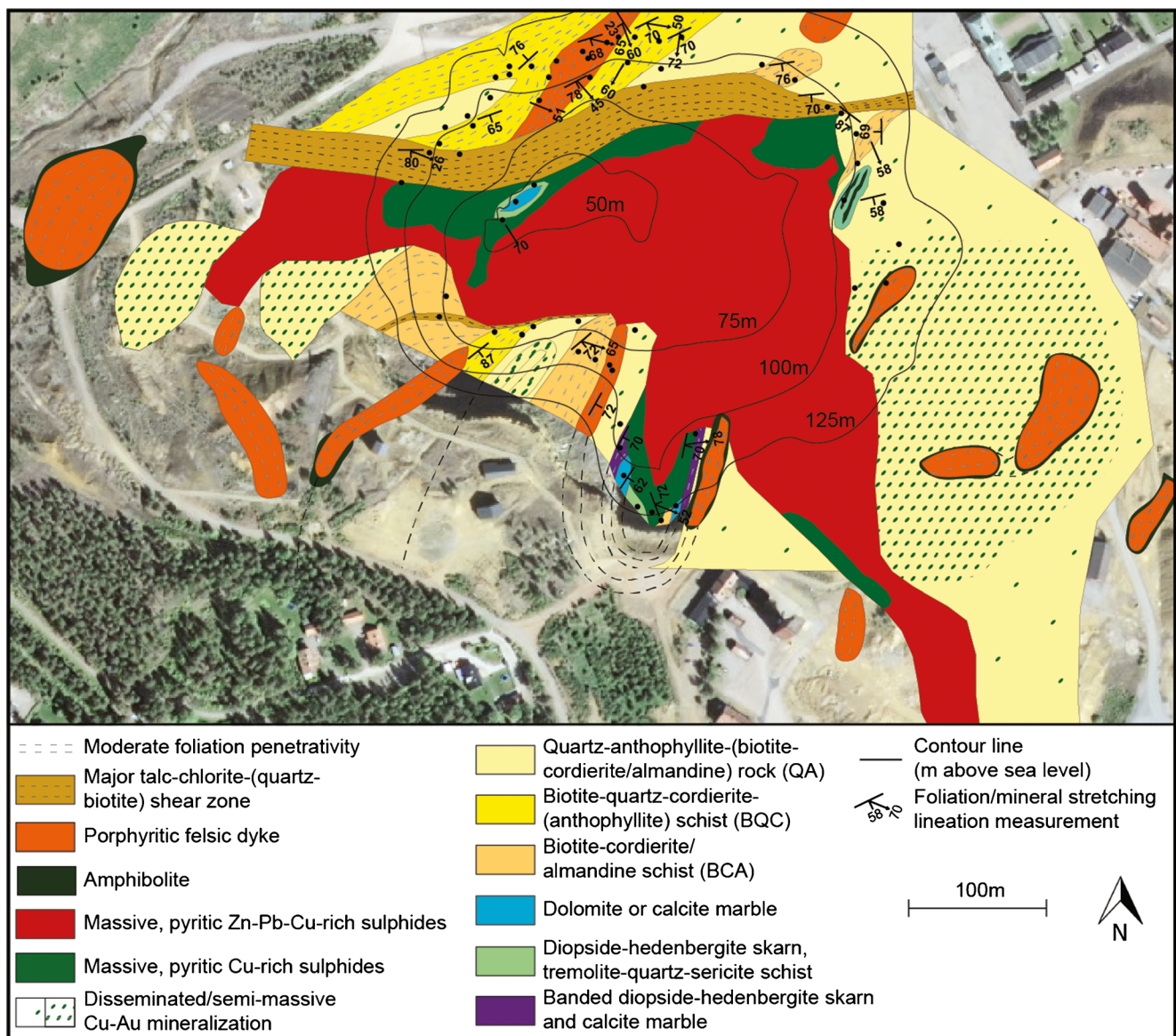
Fig. 3 Geological map of the Falun open pit at the ground surface, based on an integration of surface mapping, mine maps and drill core logging. Representative structural measurements are shown. The background is an aerial photograph, provided by Lantmäteriet, Sweden. Note the topographic difference between the outside (+140 m) and the centre of the open pit (+50 m)

bodies with sphalerite and galena (up to 5 %) are also present. Combined base metal head grades for the mineralization types excluding the massive sulphides are 2.5 % Cu, 0.5 % Zn and 0.1 % Pb (Grip 1978).

2D surface model

The previous geological mapping around the deposit combined with the new mapping in the open pit as well as core logging have provided constraints on the spatial extent of the hydrothermally altered zone at the ground surface (Fig. 3). To the east of the deposit, the boundary between the surrounding felsic sub-volcanic or volcanic rocks and the intensely altered rocks trends approximately N–S and lies ~300–400 m from

the centre of the deposit (Fig. 1b). To the south, this boundary is more irregular in orientation and extends ~800 m from the centre (Fig. 1b). On the western side of the deposit, only altered rocks have been observed in drill core, which might be due to a connection between the altered zone at Falun and the cordierite-anthophyllite-bearing, metamorphosed altered rocks associated with the Näverberg and Skyttgruvan Cu-Zn sulphide deposits, ~4 km west of Falun (Fig. 1b). There is little outcrop north of the deposit within the area of the town of Falun. In this direction, the GDG granite that bounds the inlier ~3 km north of the deposit (Fig. 1b) defines the maximum extent of the hydrothermally altered zone.

A major ductile shear zone is located in the north of the deposit (Fig. 3). This zone is ~10 m thick and strikes ENE–

WSW. The sheared rock is characterized by a talc-chlorite-(quartz-biotite) mineral association and has a brown-yellow appearance owing to the high content (~5 %) of sulphides (mainly chalcopyrite). This zone and the associated offset separate the deposit into northern and southern structural domains, thereby controlling the distribution of rock types. The northern structural domain is characterized by silicate-rich altered rocks, mainly BQC schist. The QA rock and BCA schist commonly form lenses inside larger BQC schist bodies and a porphyritic felsic dyke in the BQC schist terminates to the south along the bounding ductile shear zone (Fig. 3).

A distinguishing feature of the southern structural domain is the presence of massive sulphides, marble and skarn (Fig. 3). Lenses and fragments of marble and skarn are common at the margins to and inside the massive, pyritic sulphides (Fig. 3). The mineralized bodies in the southern structural domain are complexly zoned with an overall concentric pattern from massive, pyritic Zn-Pb-Cu-rich sulphides in the centre, surrounded successively by massive, pyritic more Cu-rich sulphides and semi-massive to disseminated Cu-Au mineralization. The massive, pyritic Cu-rich sulphides are only rarely in contact with the semi-massive Cu-Au mineralization (Fig. 3). However, it is in direct contact with the major talc-chlorite-(quartz-biotite) shear zone to the north and merges into massive Zn-Pb-Cu-rich sulphides to the south (Fig. 3).

At the ground surface, the silicate-rich altered rocks envelop the massive sulphides on both sides of the southern structural domain (Fig. 3). The QA rock, associated with disseminated to semi-massive Cu-Au mineralization to the east, west and south-west of the deposit, is generally situated proximal to the massive sulphides and is the most abundant rock type in this domain (Fig. 3). The same formation of lithological lenses between the silicate-rich altered rocks as observed in the northern structural domain is present. On the south-western side of the Zn-Pb-Cu-rich massive sulphides, the contacts to the altered rocks (NE–SW trending) appear to be structurally discordant to the orientation of the massive sulphides (WNW–ESE), although the contacts are, at least locally, sheared, indicated by the presence of minor talc-chlorite-(quartz-biotite) shear zones in this area (Fig. 3).

In the southern structural domain, porphyritic felsic dykes intruded the altered rocks on all sides of the deposit (Fig. 3) and the massive, pyritic sulphides (Geijer 1917; Koark 1962). Mapping in the Falun area showed that these dykes only occur in the vicinity of the deposit, which is consistent with earlier observations by Geijer (1917) and Koark (1962).

3D model

A 3D model for the Falun deposit is presented in Fig. 4. Notable is the occurrence of several, steeply plunging, rod-to cone-shaped bodies of massive, pyritic sulphides down to

approximately −350 m (Fig. 4). The disseminated to semi-massive, Cu-Au mineralization (Fig. 4) terminates at approximately −150 m. However, bearing in mind that the modelling is based on the available mine maps and the highly variable metal grades of this mineralization type, it cannot be ruled out that the Cu-Au mineralization continues down to lower levels, but might not have been mapped in detail due to its sub-economic character at these depths.

In the same manner as at surface (Fig. 3), bodies of disseminated to semi-massive Cu-Au mineralization and massive, pyritic Cu-rich sulphides surround the massive, pyritic Zn-Pb-Cu-rich sulphides in the central part of the deposit, i.e. there is a conspicuous cone-shaped zonation pattern (Fig. 4). Furthermore, silicate-rich altered rocks also envelop the massive sulphides on both the eastern and western sides of the massive sulphides south of the major shear zone. Silicate-rich altered rocks are by far the most abundant lithology at depth (Fig. 4), with marble and skarn only forming minor bodies spatially associated with the massive, pyritic sulphides.

The cone-shaped mineralized bodies plunge steeply to the SSE (Fig. 5a). Despite the local pinching and swelling, these bodies have essentially round shapes in horizontal section (Fig. 5b). The cones of pyritic massive sulphides generally thicken towards surface. This is most evident for the massive, pyritic Zn-Pb-Cu-rich sulphides, which, at lower elevations, consists of three to four separate rods pinching out at different depths (Fig. 5a, b). Upwards, these rods merge into a single body at about −100 m, thickening further upwards from ~90 m in diameter at −100 m to ~270 m in diameter at surface elevation of approximately +150 m (Fig. 5c).

Another conspicuous feature of the 3D model is the downwards continuation of the major ENE–WSW-striking shear zone bounding the massive sulphides on their northern side (Fig. 3). Drill core data suggests that this structure continues to form the northern boundary of the massive, pyritic Cu-rich sulphides down to the base of the deposit (Fig. 5d), which is consistent with underground observations by Gavelin (1989). Since the ductile sheared rock generally contains a high amount (up to 5 %) of sulphides, the transition between the mineralized shear zone and the massive, pyritic Cu-rich sulphides immediately to the south is somewhat diffuse.

Heterogeneity in foliation penetrativity and occurrence of ductile shear zones

Strain localization is common in the rocks at Falun. The ductile deformation in the altered rocks depends on their quartz content, the most quartz-rich QA rock being least affected (Fig. 6a). A planar grain-shape fabric defined by parallel biotite and quartz is locally developed in this lithology, which is thereby described as weakly foliated.

By contrast, the more micaceous altered rock varieties, the BQC and BCA schists, show a penetrative tectonic fabric and

Fig. 4 3D model of mineralized bodies (down to −450 m elevation), as well as altered rocks and other rock units (down to +30 m) at the Falun deposit viewed to the north. The major talc-chlorite-(quartz-biotite) shear zone is only shown down to +30 m
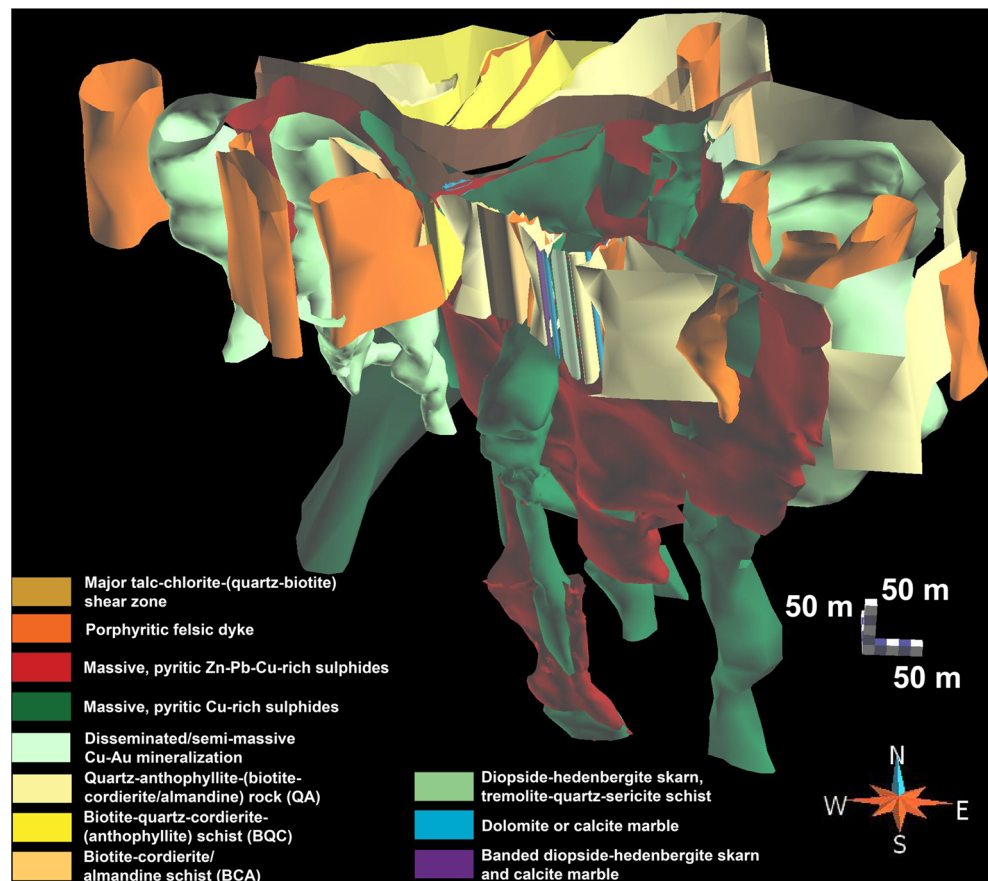
are moderately foliated (Fig. 3). The tectonic foliation in these lithologies is defined by strongly oriented grains of biotite and, to a lesser extent, quartz (Fig. 6b). A similar, moderate foliation is developed in the porphyritic felsic dykes at the deposit (Fig. 3). In the felsic rocks surrounding the deposit, heterogeneity in foliation penetrativity is expressed by the frequent occurrence of up to 0.5-mm-thick shear bands of oriented muscovite grains, and a weakly foliated groundmass of quartz, feldspar and aligned muscovite flakes leading to an overall moderately foliated appearance of the rock (Fig. 6c).

Rocks affected by shearing and a strong ductile fabric at the Falun deposit occur along mesoscopic zones with variable mineral associations. These shear zones are oriented parallel to the prominent NE–SW to E–W foliation and contribute to the marked transposition of rock units into a NE–SW orientation at the deposit (Fig. 3). The zones commonly develop along rock contacts (Fig. 7a) but also occur within the altered rocks. In, for example, the QA rock, foliation occurs along shear zones, leading to the development of mica-rich shear domains anastomosing around isotropic or weakly foliated tectonic lenses of QA rock (Fig. 6d). The mica-rich shear zones have a typical thickness of ~0.5–2 m, and the tectonic lenses show variable thicknesses from a few centimetres to several tens of metres. A second type of shear zone containing the mineral association talc-chlorite-(quartz-biotite) and

chalcopyrite occurs at a larger scale, defining the northern boundary of the massive sulphides (Figs. 3, 5d and 7b). Microstructural investigation reveals strongly stretched mineral grains in this rock (Fig. 7c). A minor talc-chlorite-(quartz-biotite) shear zone has been observed in the south-western part of the deposit, most likely bordering the massive sulphides to the south in a similar fashion (Fig. 3).

Polyphase ductile deformation and sense of ductile shear displacement

The presence of two distinct tectonic foliations, referred to here as S_1 and S_2, is indicated by structural observations and measurements at the ground surface in and around the deposit combined with microstructural analysis. Due to the poor development of tectonic fabric in the weakly foliated QA rock and the strong deformation in the ductile shear zones discussed above, the best observations of foliation development can be made in the moderately foliated, felsic rocks surrounding the deposit, and in the BQC and BCA schists at the deposit.

In the felsic rocks surrounding the deposit, S_1 is developed as a penetrative grain-shape fabric composed of elongate muscovite and biotite flakes up to 200 μm in length (Figs. 8a, b). In the groundmass of these rocks, quartz and feldspar grains also show a weak alignment parallel to this S_1 direction. In the

Fig. 5 Geometric investigation of the Falun massive sulphides in 3D. **a** Visualization of the mean plunge of the central massive, pyritic Zn-Pb-Cu-rich sulphides. **b** 3D geometry of the base rods of the massive, pyritic sulphides (−160 m to −350 m), viewed to the north. **c** Top view of the central massive, pyritic Zn-Pb-Cu-rich sulphide body, illustrating the thickening from its base at approximately −100-m elevation to the ground surface at approximately +150 m. **d** 3D spatial relationships between pyritic, massive sulphides and the major talc-chlorite-(quartz-biotite) shear zone. The mineralized ductile deformation zone is in direct contact with the massive sulphides to the north. View to the east

Major talc-chlorite-(quartz-biotite) shear zone

Massive, pyritic Cu-rich sulphides

Massive, pyritic Zn-Pb-Cu-rich sulphides
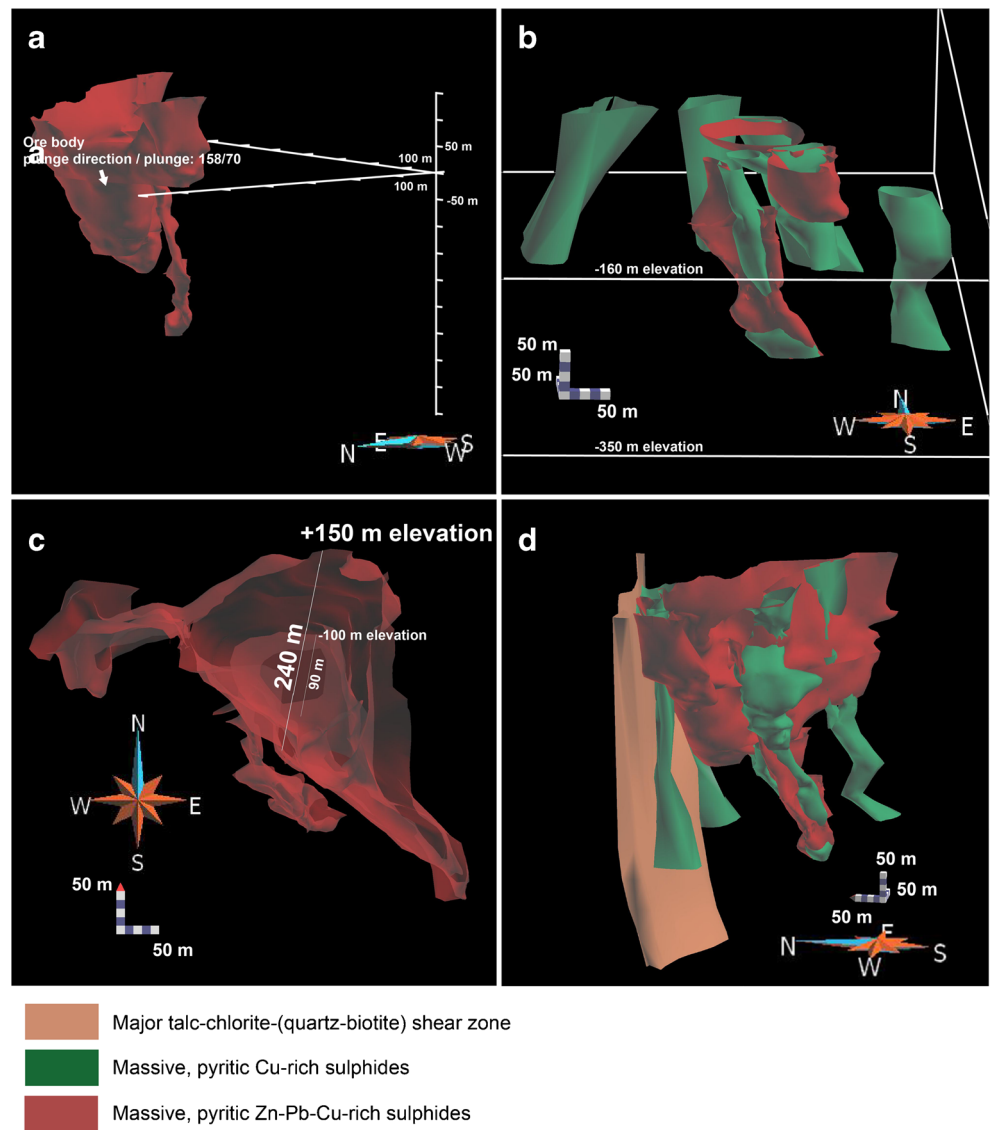
BQC and BCA schists, S_1 is preserved inside cordierite porphyroblasts being defined by strongly oriented mineral inclusions of muscovite, biotite and quartz (Figs. 8c, d).

S_2, the dominant foliation, is recognizable in different rock types at the Falun deposit. In the surrounding felsic rocks, S_2 corresponds to a spaced, planar grain-shape fabric defined by oriented biotite and muscovite (Fig. 8a). A similar spaced fabric defined by biotite-cordierite bands in the BQC schist (Fig. 8e) comprises the S_2 foliation in this lithology. In general, the contacts between rock units in the area show the same orientation as S_2 due to the pronounced D_2 transposition (Fig. 3). Ductile deformation in the major talc-chlorite-(quartz-biotite) shear zone with sulphides to the north of the massive sulphide ores (Fig. 3) is interpreted to be coupled to the later stages of the D_2 tectonic phase.

A penetrative grain-shape fabric, defined by muscovite and biotite, is also present in the porphyritic felsic dykes. This foliation locally rotates around quartz and feldspar phenocrysts in the dykes (Fig. 8f). A spaced grain-shape fabric is only occasionally present, but this may be due to the lower content of biotite and muscovite in this lithology compared to that present in the surrounding felsic rocks and in the BQC and BCA schists. It is not possible to conclude whether the ductile deformation inside the dykes is related to the development of S_1, S_2 or a combination of these two structures.

Cross-cutting relationships between S_1 and S_2 are scarce. In the majority of examined rock exposures and thin sections, S_1 is inferred to have been parallelized with S_2 due to D_2 transposition (Figs. 8a, d). However, S_2 in the groundmass of the altered rocks is locally developed at an angle to the preserved S_1 in the cordierite porphyroblasts (Fig. 8c). A mineral stretching lineation defined by stretched cordierite porphyroblasts in the BQC schist, quartz and feldspar
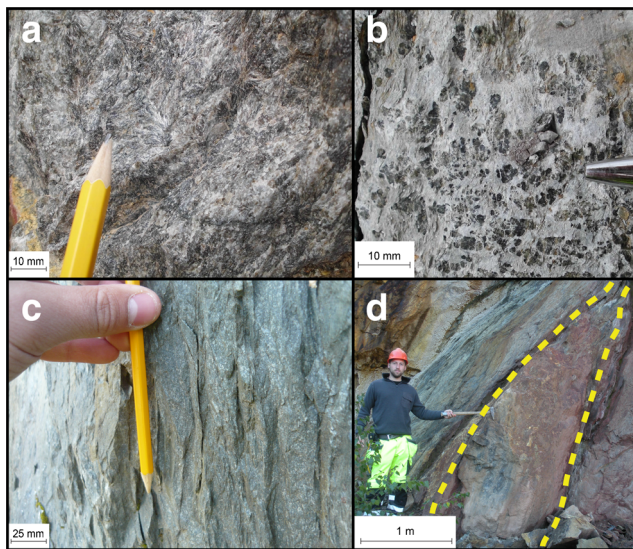
Fig. 6 Heterogeneity of foliation penetrativity at and surrounding the Falun deposit. **a** Isotropic to weakly foliated QA rock. **b** Moderately foliated BQC schist, top view. **c** Spaced foliation defined by biotite and muscovite bands in a felsic sub-volcanic or volcanic rock surrounding the deposit along a road cut west of Falun. **d** Tectonic lens of QA rock inside a mica-rich shear zone

phenocrysts in the porphyritic felsic dykes, and pyrite in the massive sulphides has been observed in the open pit. In summary, the deformation pattern at Falun is dominated by a combined planar and linear fabric (S-L fabric).

The relationships at the Falun deposit are visualized with the help of stereographic projections of structural data from the open pit (Figs. 3 and 9a). It has not been possible to confidently separate the S_1 and S_2 structures during field measurements and, for this reason, the two foliations are distinguished neither on the map (Figs. 3 and 9a) nor in the stereographic projection (Fig. 9b). Folding is scarcely recognizable at a smaller scale. However, a tight and steeply SSE-plunging fold, which deforms an earlier (S_1) tectonic fabric, was observed along a road cut ~500 m south-east of the open pit (Fig. 9c, d). The mineral stretching lineation measurements also plunge steeply towards the SSE (Fig. 9d).

The poles to foliation measurements define a best fit great circle (Fig. 9b), which is interpreted to represent folding of a S_1 planar grain-shape fabric with an inferred F_2 fold axis sub-parallel to the steep mineral stretching direction and the measured fold axis orientation (Fig. 9b, d). The majority of the poles to the foliation form a cluster with gently plunging NW trends (Fig. 9b), which most likely represents measurements of the dominant S_2 foliation developed as an axial surface foliation to the inferred F_2 fold. For this reason, the S_2 foliation is inferred to strike ENE and dip steeply to the SSE. Calculation of the Fisher mean vector to the entire foliation data (Fig. 9b) corresponds to a mean foliation plane with a dip direction and dip of 154/65 ($\alpha 95 = 8.2°$, $\kappa = 4.1$). Given the homogeneous data spread and the acceptable

Fisher statistics around the mean vector, this is considered to be an approximate estimate of the mean S_2 foliation.

Microstructural analysis of oriented samples of the mica-rich ductile shear zones reveals the presence of C'S fabrics. The S-fabric is defined by oriented muscovite and/or biotite, and the geometric relationship between these surfaces indicates consistent sub-vertical, S- to SE-side-up kinematics (Fig. 7d). The rotation of lithological contacts into the major talc-chlorite-(quartz-biotite) shear zone in the northern part of the open pit (Fig. 3) suggests a subordinate, dextral strike-slip shear component along this zone. The NW–SE strike and steep NE dip of a set of quartz veins with thicknesses of 0.1–0.3 m in a porphyritic felsic dyke north of the ductile shear zone (Fig. 7e, f) indicate a NE–SW extensional direction, consistent with a dextral strike-slip shear component (Fig. 7f).

Relationships between ductile deformation and mineral growth or recrystallization

Textural and microstructural investigations at Falun provide the basis for an interpretation of the temporal relationships between ductile deformation and mineral growth or recrystallization at the deposit. Some critical relationships are shown in Fig. 10, and a summary of the relative timing of mineral growth or recrystallization and the two main phases of ductile deformation (D_1 and D_2) is presented in Fig. 11.

Quartz exists in the QA rock and BQC schist both as a medium- to coarse-grained phase in the groundmass (Figs. 8d and 10a) and as fine-grained inclusions in cordierite porphyroblasts (Figs. 8c and 10a). When present in the groundmass, quartz is usually statically recrystallized and shows no intracrystalline deformation (Fig. 8a, b). This process led to an increase in grain size to 300 to 1000 μm for groundmass quartz compared to quartz and biotite inclusions inside cordierite with a grain size of 10 to 100 μm (Fig. 8d). In the QA rock and BQC schist, quartz grains are variably elongate in the directions of S_1 and S_2 as mineral inclusions and groundmass minerals, respectively (Fig. 8c, d). Quartz was most likely a mineral component in the rocks at Falun before the tectonothermal phase but later grew and recrystallized during D_1 and D_2 and possibly between these two deformational events (Fig. 11), leading to the strongly increased grain size in the groundmass.

Biotite shows a similar grain size as quartz in the groundmass of the QA rock and BQC schist, which is probably due to the same grain size increase by static recrystallization as for quartz (Figs. 8d, e and 10a). In the silicate-rich altered rocks, biotite is usually spatially associated with cordierite and, together, these minerals form foliation bands between quartz-rich bands of similar thickness of 200 μm to 1 mm (Figs. 8e and 10a). The intimate intergrowth suggests formation during the same tectonic event. Groundmass biotite forms elongate
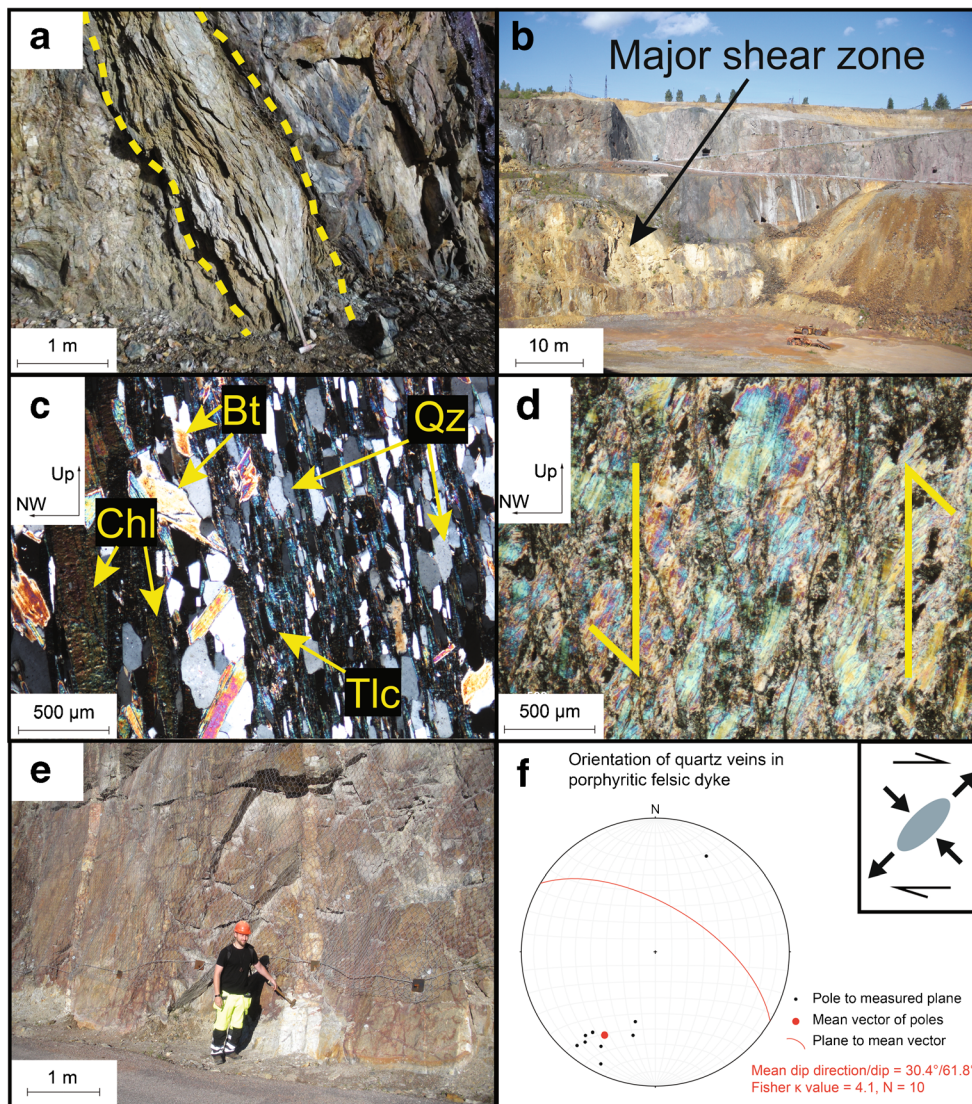
Fig. 7 Ductile deformation along shear zones in the Falun open pit. **a** Mica-rich shear zone (central part of photograph) defining a tectonic contact between a BQC schist (*left*) and a porphyritic felsic dyke (*right*). **b** View of the northern side of the Falun open pit showing a major ductile shear zone weathered in a yellowish colour containing the mineral association talc-chlorite-(quartz-biotite) with sulphides, mainly chalcopyrite (Fig. 3). **c** Microphotograph (cross-polarized light) of an oriented rock sample of the shear zone shown in Fig. 7b. Stretched mineral grains of biotite (partly chloritized), talc and quartz demonstrate strong shearing. Abbreviations: Bt = biotite, Chl = chlorite, Qz = quartz, Tlc = talc. **d** Microphotograph (cross-polarized light) of an oriented thin section of the shear zone in Fig. 7a. C'S fabric indicates S-side-up sense of shear. **e** Quartz veins in a porphyritic felsic dyke on the northern side of the Falun open pit. **f** Stereographic projection of poles to measured orientations of the set of quartz veins in Fig. 7e. Plane corresponding to the mean vector of the poles (i.e. the mean orientation of quartz veins) dips steeply to the NE, which is perpendicular to the inferred extensional direction in a dextral strike-slip kinematic setting

grains generally parallel to S_2 but also rotated into the S_2 foliation. Locally, grains of biotite have been observed in cordierite porphyroblasts (Fig. 10b), suggesting growth or recrystallization also prior to the growth of cordierite during development of the S_1 foliation. Muscovite shares a similar growth history with biotite. It records D_1 as mineral inclusions in cordierite (Fig. 8c, d) and defines both the penetrative S_1 and the spaced S_2 fabric in the felsic rocks surrounding the deposit (Fig. 8a, b). It is inferred that both biotite and muscovite grew during both D_1 and D_2 as well as between these two events (Fig. 11).

In the BCA schist, strongly foliated (S_2) biotite bands bend around commonly retrogressed almandine porphyroblasts (Fig. 10c) with a grain size ranging from 10 μm to 100 mm. These porphyroblasts commonly show signs of rotation in the biotite groundmass due to ductile shearing along S_2. The almandine is inferred to have grown between D_1 and D_2 (Fig. 11).

Cordierite porphyroblasts (Fig. 10a, b) are a prominent mineral in the silicate-rich altered rocks. They commonly form boudinaged, rosette-like garben textures on the main (S_2) foliation planes. Similar to almandine, cordierite is
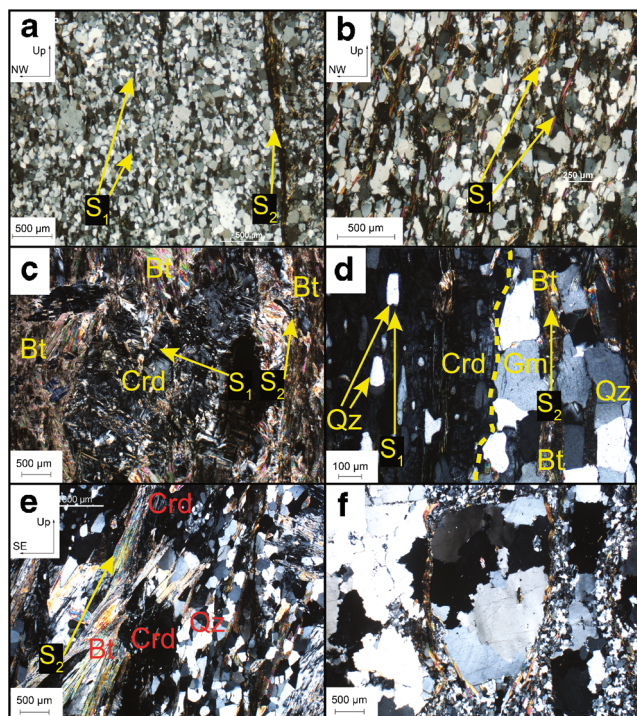
Fig. 8 Microphotographs (cross-polarized light) of different lithologies at Falun showing polyphase ductile deformation. **a** Penetrative (S_1) and spaced (S_2) tectonic foliations, defined by muscovite and biotite flakes and bands, respectively, in a fine-grained, felsic rock surrounding the deposit along a road cut west of Falun (see Fig. 6c). **b** Close-up showing the character of the S_1 tectonic foliation in the felsic rock in Fig. 8a. **c** S_1 foliation defined by inclusions of muscovite in a cordierite porphyroblast in a BCA schist from the north-eastern side of the Falun open pit. A later S_2 foliation is defined by statically recrystallized biotite in the surrounding groundmass. **d** S_1 foliation defined by inclusions of quartz in a cordierite porphyroblast in a BQC schist from the northern side of the Falun open pit. A later S_2 foliation, here parallel to S_1, is defined by statically recrystallized, coarser-grained biotite and quartz in the surrounding groundmass. **e** Spaced S_2 foliation in a BQC schist, defined by alternating bands of biotite-cordierite and quartz. **f** Tectonic foliation, defined by biotite and muscovite, enveloping a quartz phenocryst in a porphyritic felsic dyke. Abbreviations: Bt=biotite, Crd=cordierite, Gm=groundmass, Qz=quartz

inferred to have grown between D_1 and D_2 (Fig. 11). Since the cordierite porphyroblasts in the BQC schist are stretched and provide a basis for the measurement of the mineral stretching lineation in the area, the latter is inferred to be, at least partly, a L_2 structure.

Andalusite occurs as a minor portion of porphyroblasts in the QA rock, especially in the eastern and north-eastern part of the open pit. Due to their occurrence in this weakly foliated altered rock, their growth relationship to the ductile deformation is not clear. However, cordierite porphyroblasts have been observed inside andalusite, which also shows thin rims of cordierite and chlorite. Growth of andalusite simultaneously to or after cordierite and almandine but prior to the D_2 event is inferred.

Anthophyllite typically forms elongate fan- to sun-shaped crystals of 100-μm to 200-mm length. In the QA rock and BQC schist, anthophyllite characteristically nucleates in

foliation bands of quartz and grows in random orientations. The crystal needles crosscut the S_2 foliation, as well as several of the previously described major rock-forming minerals in the altered rocks (Fig. 10d). However, growth relationships between anthophyllite and almandine could not be observed, which is probably caused by the limited occurrence of almandine in the QA rock and BQC schist. Anthophyllite also grows over groundmass chlorite. The anthophyllite porphyroblasts are inferred to have grown after D_2 deformation ceased, but may have nucleated during D_2 (Fig. 11).

Discussion

Revised structural model involving sheath folding

The orientation of the foliation dominated by S_2 (dip direction and dip = 154/65), the inferred F_2 fold axis (151/70) and the mean L_2 mineral stretching lineation (133/69) (Fig. 9b, d), all steep to the SSE, coincide well with the overall linear trend of the mineralized bodies at Falun (158/70, Fig. 5a). The structural data set indicates the presence of a megascopic, steeply SSE-dipping, F_2 reclined fold that deformed the mineralized bodies, the altered rocks and the S_1 fabric, the dip direction of the axial surface to the fold being sub-parallel to the fold axis. Furthermore, these structures are similar in orientation to a sub-vertical stretching component, marked at the largest scale by the cone- or rod-like geometries of the mineralized bodies, which pinch and swell and generally thin down at depth. The results of this study highlight the significance of the D_2 structures for understanding the geometry of the different types of mineralization and altered rocks at the Falun deposit and are in general agreement with Weijermars (1987, unpublished mine report).

Based on the 3D model for the Falun deposit, a concentric pattern for the different mineralization types can be observed in the southern structural domain, disseminated or semi-massive Cu-Au mineralization in the outer part passing successively to massive Cu-rich sulphides and massive Zn-Pb-Cu-rich sulphides, both pyritic, in the inner part (Figs. 3 and 4). Furthermore, altered rocks of similar character occur around the deposit (Fig. 3). The formation of one or several F_2 sheath folds enriched in sulphides at the deposit, incorporating the reclined fold geometry discussed above, is suggested as an explanation for these concentric patterns that developed perpendicular to the stretching direction. The occurrence of sheath folds has been reported previously in the Outokumpu ore district in the Fennoscandian Shield (Park 1988) as well as in other Precambrian ore districts affected by ductile deformation and metamorphism such as Itabira in Brazil (Giuliani et al. 1990; Olivo et al. 1995), the Manitouwadge greenstone Belt in Canada (Zaleski and Peterson 1995) and Broken Hill in Australia (Forbes et al. 2004).

Fig. 9 Structural orientation data at the Falun open pit. **a** Vertical aerial photograph of the Falun open pit (provided by Lantmäteriet, Sweden) with locations of structural measurements shown as black dots. **b** Stereographic projection of poles to foliation measurements. The pole to the best fit great circle (inferred fold axis of the megascopic fold structure) is shown. The Fisher mean vector to the entire foliation data corresponds to a mean foliation plane with a dip direction and dip of 154/65 ($\alpha95 = 8.2°$, $\kappa = 4.1$). **c** Macroscopic fold structure in a road cut ~500 m south-east of the Falun open pit, viewed in a sub-vertical direction. **d** Stereographic projection of mineral stretching lineations measured in the Falun open pit and their mean vector. The measured axis of the fold in Fig. 9c is also shown
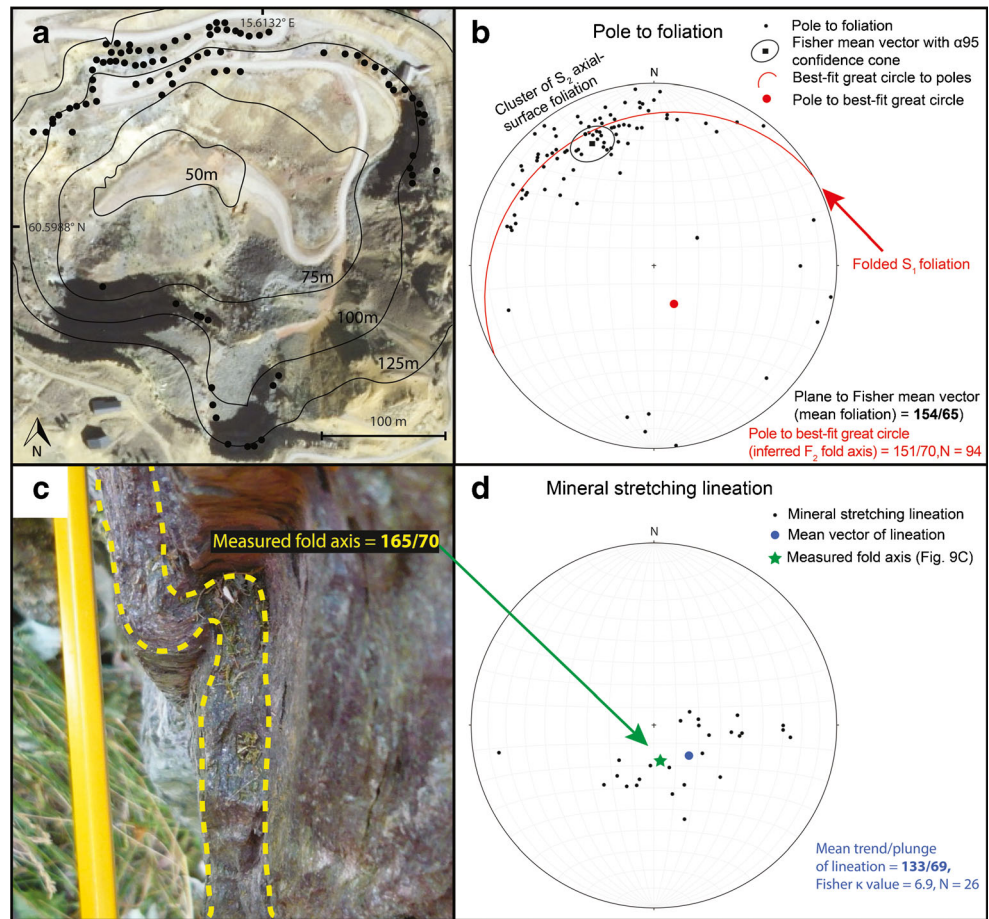
A sheath fold is a highly non-cylindrical fold in which the hinge curvature exceeds 90° within the axial surface (Cobbold and Quinquis 1980; Skjernaa 1989). Although sheath folds have been shown to form under pure and general shear at varying scales with wavelengths from less than 1 mm to several kilometres (Alsop and Holdsworth 2006), a strong simple shear component is considered the most important bulk strain type to form these structures (Van der Pluijm and Marshak 2004; Fossen 2010). Generally, the development of high-strain bulk simple shearing, stretching lineation and mylonitic fabric seems to represent favourable conditions for sheath fold formation (Cobbold and Quinquis 1980). Besides the presence of a S-L fabric including a mineral stretching lineation and stretched rod-like geometries for the different mineralization types, our study has shown that the Falun deposit is associated with extensive shearing that involved a strong simple shear component, with the development of ductile shear zones bounding the mineralized bodies, shearing along lithological contacts and tectonic lensing.

Using analogue modelling, Marques et al. (2008) showed that high-strain, non-passive folding involving rock layers or units with rheological contrasts results in sheath folding of the rock unit with the lower viscosity and that the magnitude of the viscosity contrast (μ') determines the ductile behaviour of the more competent rock unit. At low viscosity contrasts ($\mu' < 10$), this unit would also form a sheath fold around the lower competent unit. At high viscosity contrasts, the competent unit would effectively behave as a rigid body and respond to the high strain only by translational movement (Marques et al. 2008). The latter case can most likely be applied to the deformation at the Falun deposit. A high viscosity contrast is predicted between the central massive sulphides and the surrounding quartz-rich QA rock (Figs. 3 and 4). The isotropic to weakly foliated character of the QA rock indicates that this rock type acted as a rigid frame, in the centre of which pronounced tubular sheath folds of sulphides could develop.

The previous structural model used to explain the geometry of the Falun deposit (Koark 1962, 1973) involved a dome-and-basin structure corresponding to the Type 1 refolded fold pattern of Ramsay (1967). Concentration of the sulphides in the hinge zone of the second generation fold and the presence of barren rocks to the south-west of the deposit were inferred. The occurrence of steeply plunging sheath folds with a strong simple shear component formed during a single phase of folding (F_2), suggested here, questions the traditional structural model for Falun and suggests the presence of the same stratigraphic unit (stratigraphic footwall) on all sides of the deposit.
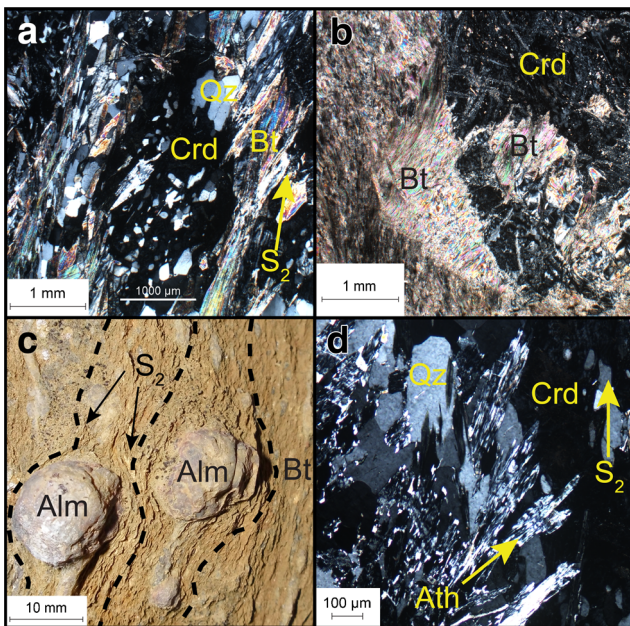
Fig. 10 Major rock-forming minerals in the silicate-rich altered rocks at the Falun deposit. **a** Cordierite porphyroblast with fine-grained quartz inclusions in a BQC schist (cross-polarized light). **b** Biotite fragment inside a cordierite porphyroblast (cross-polarised light). **c** Porphyroblasts of almandine in a biotite-dominated matrix in a BCA schist. Foliation (S$_2$) bands of biotite bend around the porphyroblasts. **d** Needle- to fan-shaped anthophyllite growing over quartz and cordierite porphyroblasts and cross-cutting the S$_2$ foliation (cross-polarized light). Abbreviations: Alm = almandine, Ath = Anthophyllite, Bt = biotite, Crd = cordierite, Qz = quartz

Koark (1973) compared the length relationships between long (sub-vertical) and short (sub-horizontal) axes of 22 polymetallic sulphide bodies in Bergslagen and inferred an average ratio of 2.5:1. Considering that denudation might have eroded upper portions of the mineralized bodies, this estimation is probably a minimum value. These observations suggest that base metal sulphide and possibly even iron oxide deposits in Bergslagen have been subject to strong, steeply plunging stretching. Stretched, cone-to rod-shaped geometries for both base metal sulphide and Fe-oxide mineralizations have been described at numerous deposits in the Bergslagen

Fig. 11 Relative timing between D$_1$ and D$_2$, the intermediate static period and the growth or recrystallization of the major rock-forming minerals (black lines) in the silicate-rich altered rocks at the Falun deposit

ore district, such as at the Garpenberg base metal sulphide deposit (Allen et al. 2003, unpublished research report) and the iron oxide deposits at Kärrgruvan (Hjelmqvist 1942; Koark 1973) and Grängesberg (Högdahl et al. 2013). At Garpenberg, the deformation pattern was linked to F$_2$ folds described as cone- or funnel-shaped that refolded an older, major F$_1$ fold, i.e. two phases of folding, as proposed earlier for Falun and even other deposits (Carlon and Bleeker 1988) in the district. This is in contrast to the single phase of folding with progressive development into a sheath fold (F$_2$) proposed here for Falun.

Polyphase ductile deformation in a regional structural and metamorphic context

An early major folding event (F$_1$), locally with large-scale stratigraphic inversion of the bedrock, has been recognized in parts of the Bergslagen lithotectonic unit, but a second generation of folding (F$_2$), with deformation of the regional planar grain-shape fabric and continued development of linear structures, is the most prominent structural feature (Stephens et al. 2009, Beunk and Kuipers 2012). The second generation of folding is apparent on different scales, including the regional scale (Fig. 1a).

The D$_1$ and D$_2$ structures identified in this study fall well within this regional pattern and are inferred to have formed during the separate pulses of transpressive deformation at the closing stages of the two tectonic cycles recognized within the Bergslagen lithotectonic unit (Stephens et al. 2009; Beunk and Kuipers 2012; Stephens and Andersson 2015). Beunk and Kuipers (2012) included the two phases of transtensional or extensional strain prior to and between the major phases of transpressional ductile fabric development and folding in their structural evolutionary scheme; D$_1$ and D$_2$ in this study corresponding to their D$_2$ and D$_4$, respectively.

The Falun deposit is situated on the north-western limb of a major, generally east-plunging synform inside the central part of the Bergslagen lithotectonic unit (Fig. 1a), formed during the regional, D$_2$ deformational event (Stephens et al. 2009). The presence of such a major fold structure predicts the development of strong ductile shearing with parasitic fold structures along its limbs. Kinematic indicators at Falun suggest a transpressive regime with S- to SE-side up and subordinate dextral movement, the dip-slip component consistent with the sense of displacement along steeply dipping, ductile shear zones with NE–SW strike south-east and south of Falun (Allen et al. 2003, unpublished research report, Beunk and Kuipers 2012). Thus, the results of this study, demonstrating the presence of dominant, steeply SSE-plunging F$_2$ structures at Falun, fit into the regional expression of D$_2$. The transpressive D$_2$ regime led to significant transposition and overprinting of the D$_1$ structures, so that S$_1$ and S$_2$ are commonly close in orientation to each other.

It has previously been suggested that metamorphism under lower amphibolite-facies conditions isochemically modified the mineralogy of the hydrothermally altered rocks at the Falun deposit (Wolter and Seifert 1984). The results presented here show that the major rock-forming minerals in the silicate-rich altered rocks at Falun have grown or recrystallized during or between different phases of the deformational evolution and, consequently, support the conclusion drawn by Wolter and Seifert (1984). There are also clear similarities to the results of a similar study conducted at the Stollberg Fe-Pb-Zn-Mn-(Ag) deposit, situated ~50 km south of the Falun deposit (Ripa 2012). These similarities include the continuous D_1 to D_2 growth of biotite, the post-D_1/pre-D_2 growth of andalusite and cordierite, and the post-D_2 growth of gedrite, a ferromagnesian amphibole in the same series as anthophyllite, at the Stollberg deposit.

Conclusions

The rocks at the Falun deposit have been affected by polyphase ductile deformation (D_1 and D_2). Rheological contrasts between different silicate-rich altered rocks led to localization of foliation in mica-rich altered rock and along ductile shear zones. The presence of D_2 structures that plunge steeply to the SSE are consistent with the location of the Falun deposit on the north-western limb of a regional-scale, major F_2 synform plunging eastwards.

Sheath folding along steep F_2 fold axes is suggested to be the key deformation mechanism affecting the hydrothermally altered and the mineralized rocks at the Falun deposit, leading to horizontally concentric patterns of metal zonation. The 3D model of the deposit established in this study reveals that steep stretching during ductile deformation led to cone- or rod-shaped geometries of mineralization, which thin and pinch out at depth. According to this structural model, the same stratigraphic unit (stratigraphic footwall) to the massive sulphides, with exploration potential for associated Cu-Au mineralization, is exposed on all sides of the deposit. The new model questions the traditional structural model for Falun of refolded folding. If the sheath fold model is applicable to other deposits in the Bergslagen ore district, for which a good stratigraphic control has not been established, parts that were previously considered as barren hangingwall rocks may have a higher prospectivity for base metals than previously thought.

The rock-forming minerals in the silicate-rich altered rocks at Falun are metamorphic in origin and show growth patterns during different phases of the polyphase tectonic evolution. Growth of cordierite, almandine and andalusite porphyroblasts, as well as static recrystallization of groundmass quartz and biotite, occurred between D_1 and D_2.

References

Åberg A, Fallick AE (1993) A fluid inclusion and light element stable isotope study of the gold-bearing quartz vein system, Falun, Sweden. Mineral Deposits 28:324–333

Allen RL, Lundström I, Ripa M, Simeonov A, Christofferson H (1996) Facies analysis of a 1.9 Ga, continental margin, back-arc, felsic caldera province with diverse Zn-Pb-Ag-(Cu-Au) sulphide and Fe oxide deposits, Bergslagen region, Sweden. Econ Geol 91:979–1008

Alsop GI, Holdsworth RE (2006) Sheath folds as discriminators of bulk strain type. J Struct Geol 28:1588–1606

Beunk FF, Kuipers G (2012) The Bergslagen ore province, Sweden: review and update of an accreted orocline, 1.9-1.8 Ga BP. Precambrian Res 216–219:95–119

Bromley-Challenor MD (1988) The Falun supracrustal belt. Part 1: primary geochemical characteristics of Proterozoic metavolcanics and granites. Geol Mijnb 67:239–253

Carlon CJ, Bleeker W (1988) The geology and structural setting of the Håkansboda Cu-Co-As-Sb-Bi-Au deposit and associated Pb-Zn-Cu-Ag-Sb mineralization, Bergslagen, central Sweden. Geol Mijnb 67:279–292

Cobbold PR, Quinquis H (1980) Development of sheath folds in shear regimes. J Struct Geol 2:119–126

Forbes CJ, Betts PG, Lister GS (2004) Synchronous development of Type 2 and Type 3 fold interference patterns: evidence for recumbent sheath folds in the Allendale Area, Broken Hill, NSW, Australia. J Struct Geol 26:113–126

Fossen H (2010) Structural Geology. Cambridge University Press, New York

Gavelin S (1989) Genesis of the Falun sulphide ores, central Sweden. GFF 111:213–227

Geijer P (1917) Falutraktens berggrund och malmfyndigheter. Geological Survey of Sweden, Series C 275, Stockholm

Geijer P (1964) On the origin of the Falun type of sulphide mineralization. GFF 86:3–27

Giuliani G, Silva LJHD, Couto P (1990) Origin of emerald deposits of Brazil. Mineral Deposit 25:57–64

Grip E (1978) Sweden. In: Bowie HSU, Kvalheim A, Haslam HW (eds) Mineral deposits of Europe, volume 1: Northwest Europe. Institution of Mining and Metallurgy and Mineralogical Society, London, pp 93–198

Hermansson T, Stephens MB, Corfu F, Andersson J, Page L (2007) Penetrative ductile deformation and amphibolite-facies metamorphism prior to 1851 Ma in the western part of the Svecofennian orogen, Fennoscandian Shield. Precambrian Res 153:29–45

Hermansson T, Stephens MB, Corfu F, Page LM, Andersson J (2008a) Migratory tectonic switching, western Svecofennian orogen, central Sweden: constraints from U/Pb zircon and titanite geochronology. Precambrian Res 161:250–278

Hermansson T, Stephens MB, Page LM (2008b) $^{40}Ar/^{39}Ar$ hornblende geochronology from the Forsmark area in central Sweden:

constraints on late Svecofennian cooling, ductile deformation and exhumation. Precambrian Res 167:303–315

Hjelmqvist S (1942) Stribergs malmfält. Geologisk beskrivning. Geological Survey of Sweden Series C 449, Stockholm

Högdahl K, Troll V, Persson Nilsson K, Jonsson E (2013) Structural evolution of the apatite-iron oxide deposit at Grängesberg, Bergslagen, Sweden. Proceedings of the 12th SGA biennial meeting, Uppsala: 1650–1653

Koark HJ (1962) Zur Altersstellung und Entstehung der Sulfiderze vom Typus Falun. Geol Rundsch 52:123–146

Koark HJ (1973) Zur Entstehung des tektonischen Stengelbaus an präkambrischen Eisen und Sulfiderzkörpern der zentralschwedischen Leptitserie. Mineral Deposit 8:19–34

Magnusson NH (1950) Zinc and lead deposits of central Sweden. Proceedings of the International Geological Congress 1948, Part VII: 371–379

Magnusson NH (1953) Malmgeologi. Jernkontoret, Stockholm

Marques FO, Guerreiro SM, Fernandes AR (2008) Sheath fold development with viscosity contrast: analogue experiments in bulk simple shear. J Struct Geol 30:1348–1353

Olivo GM, Gauthier M, Bardoux M, de Sa EL, Fonseca JTF, Santana FC (1995) Palladium-bearing gold deposit hosted by Proterozoic Lake Superior-type iron-formation at the Cauê iron mine, Itabira district, southern Sao Francisco Craton, Brazil: geologic and structural controls. Econ Geol 90:118–134

Park AF (1988) Geometry of sheath folds and related fabrics at the Luikonlahti mine, Svecokarelides, eastern Finland. J Struct Geol 10:487–498

Ramsay JG (1967) Folding and Fracturing of Rocks. McGraw-Hill, New York

Ripa M (2012) Metal zonation in alteration assemblages at the volcanogenic Stollberg Fe-Pb-Zn-Mn(−Ag) skarn deposit, Bergslagen, Sweden. GFF 134:317–330

Skjernaa L (1989) Tubular and sheath folds: definitions and conceptual models for their development, with examples from the Grapesvare area, northern Sweden. J Struct Geol 11:689–703

Stephens MB, Andersson J (2015) Migmatization related to mafic underplating and intra- or back-arc spreading above a subduction boundary in a 2.0–1.8 Ga accretionary orogen, Sweden. Precambrian Res 264:235–237

Stephens MB, Weihed P (2013) Tectonic evolution and mineral resources in the Fennoscandian Shield, Sweden. In: Allen RL, Jansson N, Ripa M (eds.) Bergslagen: Geology of the volcanic- and limestone-hosted base metal and iron oxide deposits, Excursion Guidebook Swe 4. Proceedings of the 12th Biennial SGA Meeting 2013, Uppsala, pp 10–20

Stephens MB, Ripa M, Lundström I, Persson L, Bergman T, Ahl M, Wahlgren CH, Persson PO, Wickström L (2009) Synthesis of the bedrock geology in the Bergslagen region, Fennoscandian Shield, south-central Sweden. Geological Survey of Sweden, Series Ba 259, Uppsala

Tegengren FR (1924) Sveriges ädlare malmer och bergverk. Geological Survey of Sweden, Series Ca 17, Stockholm

Trägårdh J (1991) Metamorphism of magnesium-altered felsic volcanic rocks from Bergslagen, central Sweden. A transition from Mg-chlorite- to cordierite-rich rocks. Ore Geol Rev 6: 485–497

Van der Pluijm BE, Marshak S (2004) Earth Structure: an Introduction to Structural Geology and Tectonics. WW Norton, New York

Wolter HU, Seifert F (1984) Mineralogy and genesis of cordierite-anthophyllite rocks from the sulfide deposit of Falun, Sweden. Lithos 17:147–152

Zaleski E, Peterson VL (1995) Depositional setting and deformation of massive sulfide deposits, iron-formation, and associated alteration in the Manitouwadge greenstone belt, Superior Province, Ontario. Econ Geol 90:2244–2261